Two-channel high-resolution quasi-monochromatic X-ray imager for Al and Ti plasma

A. Do, M. Briat, S. Baton, M. Krumrey, L. Lecherbourg, B. Loupias, F. Perez, P. Renaudin, C. Rubbelynck, Ph. Troussel

Two-channel high-resolution quasi-monochromatic X-ray imager for Al and Ti plasma.

A. Do[1, 2], M. Briat[1], S.D. Baton[2], M. Krumrey[3], L. Lecherbourg[1], B. Loupias[1], F. Pérez[2], P. Renaudin[1], C. Rubbelynck[1], Ph. Troussel[1]

[1]*Commissariat à l'Énergie Atomique, DAM-Île de France, BP 12, 91680 Bruyères-les-Châtel, France*

[2]*LULI-CNRS, École Polytechnique, CEA: Université Paris-Saclay ; UPMC Univ. Paris 06 : Sorbonne Universités, F-91128 Palaiseau cedex, France*

[3]*Physikalisch-Technische Bundesanstalt (PTB), Abbestr. 2-12, 10587 Berlin, Germany*

High-resolution, high-sensitivity X-ray imaging is a real challenge in High-Energy Density Plasma (HEDP) experiments. We present an improved design of the FUHRI (Fresnel Ultra High-Resolution Imager) instrument). Using an Ultra-High-Intensity (UHI) laser to generate hot and dense plasma in a small volume of an Al-Ti mixed target provides simultaneous imaging of both Al and Ti X-ray emission. Specifically, the Al He_β (or Ly_β) and the Ti He_α lines are imaged with a resolution of (2.7±0.3) µm and (5.5±0.3) µm, respectively. It features two transmission Fresnel phase zone plates fabricated on the same substrate, each associated with a multilayer mirror for spectral selection. Their spatial resolution has been measured on the PTB synchrotron radiation facility laboratory at BESSY II and on the EQUINOX laser facility. Results obtained on an UHI experiment highlight the difference of emission zone sizes between Al and Ti lines and the versatility of this instrument.

I. Introduction

Ultra-short laser pulses offer plasma conditions relevant to stellar opacities[1], atomic physics in general[2, 3] and topics associated to inertial confinement fusion[4]. Experiments have been conducted on the LULI2000 laser facility (LULI, CNRS, Ecole Polytechnique)[5] with an Ultra-High-Intensity (UHI) laser delivering 10^{17} to 10^{19} W.cm^{-2} on target to create plasmas with temperatures of several 100 eV and densities higher than 1 g.cm^{-3}, although only within a limited volume. These campaigns thus required a high-resolution monochromatic X-ray imager to characterize the plasma emission. FUHRI (Fresnel Ultra High-Resolution Imager) is an x-ray imager with a demonstrated resolution lower than 5 µm for an energy bandwidth limited to 100 eV centered around the Al He_β line at 1860 eV. It consists in a transmission Fresnel phase zone plate[6] (FZP) associated to a multilayer (ML) mirror for spectral selection. The present article describes an advanced version, FUHRIx2, featuring two channels each based on the FUHRI principle. The first one, "Al", identical to the previous configuration, images the Al He_β line while the second, "Ti", images the He_α line of titanium at 4750 eV with 100 eV bandwidth.

The FUHRIx2 design is detailed in section II, followed by measurements of its FZP resolutions and ML mirror reflectance on a synchrotron facility (section III) and on a laser facility (section IV). Section V presents first results obtained on an UHI experiment.

II. FUHRIx2 presentation

The FUHRIx2 diagnostic is based on the high-resolution quasi-monochromatic x-ray imager FUHRI design presented in a previous paper[7]. The FUHRIx2 chip has two FZP engraved on the same silicon substrate for simultaneous imaging at two photon energies (Figure 1). Adding another channel to the diagnostic was a necessity for the UHI experiment as the experimental target were composed of a mixed material of Al and Ti. These two line self-emission image are characteristics of two different plasma temperatures and can be analyzed along with spectroscopic data.

FZPs are focusing optics that can operate in the X-ray domain[8]. They consist of a circular transmission grating: alternating N concentric transparent and opaque zones[9,10]. The FZPs for FUHRIx2 are manufactured using an electroplating method by Applied Nanotools INC[11]. Their central area features a beam block (see *Figure 1*) to prevent direct emission[7] (i.e. the 0th order) to reach the detector.

One FZP was designed for the Al He_β line (1860 eV) or Al Ly_β line (2050 eV, Table 1) and the other for the He_α line emission of Ti (~4700 eV, Table 1). Both the central beam block surface and the surface outside the FZPs are covered by a 3 µm electroplated gold layer to stop most of the hard x-rays. Both images are detected by a Princeton PI-MTE CCD camera.

The focal distance (f_λ) of a FZP is directly linked to the wavelength of the X-rays:

$$f_\lambda = \frac{\lambda}{{r_1}^2} \quad (1)$$

where r_1 is the first zone radius and λ the considered wavelength.

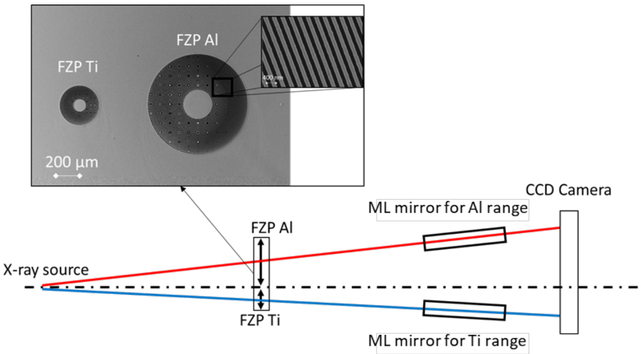

Figure 1 : FUHRIx2 setup. The two channels correspond to the Al and Ti emission focused on the CCD camera after spectral selection by ML mirrors. The top panel show a photograph of the substrate with the two FZPs.

Metrology studies were already performed to measure the Al FZP efficiency on a synchrotron radiation facility. To complete those data, additional resolution measurements have been conducted for the FZP both on a synchrotron radiation facility and on a laser facility (EQUINOX).

	FZP type	Al (1860 eV)	Ti (4700 eV)
FZP	Focal distance (f_λ)	250 mm	
	Last zone width (Δr_n)	(200 ± 5) nm	
	Diameter (D)	846 µm	330 µm
	Number of zones	1058	412
Substrate	Material	Au	
	Central stop	Au (thickness: 3 µm; diameter: 240 µm)	Au (thickness: 3 µm; diameter: 110 µm)
	Zone thickness	620 nm	
	Membrane	Si_3N_4 (100 nm thickness)	
	Support	Si wafer (10 mm x 10 mm x 0,2 mm)	

Table 1: FZPs characteristics

III. Metrology on a synchrotron radiation facility

The metrology of the components was performed at the Four-Crystal Monochromator (FCM) beamline in the Physikalisch-Technische Bundesanstalt (PTB) laboratory at the synchrotron radiation facility Bessy II[1]. The accessible photon energy range of this beamline extends from 1.75 keV to 11 keV using either Si or InSb crystals as monochromator. The zone plates were placed in an ultra-high-vacuum reflectometer[2], which provides 0.001° angular resolution for the sample and the detector.

1. FZP spatial resolution

Resolution measurement method

The resolution of the FZP was measured with the knife edge method (cf. Figure 2). The monochromatic beam was collimated to have a size of 0.5 mm x 0.5 mm. First, the piezo-blade covers all the synchrotron beam signal. Then it is removed gradually (Figure 2), with a step size of 1 µm or 0.2 µm, to reveal the focal spot until it totally gets out of the beam. The signal was recorded using an 8 mm diameter photodiode.

The resolution is obtained as the full width at half maximum (FWHM) of the derivative of the measured signal as a function of blade position. An example of such a result for the Al FZP of FUHRIx2 is presented on Figure 3.

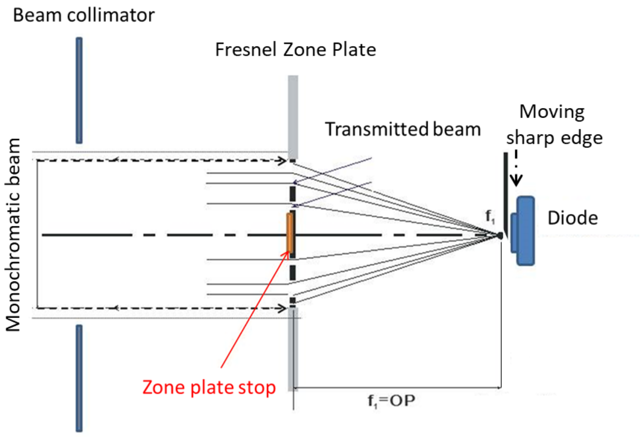

Figure 2: Knife edge method

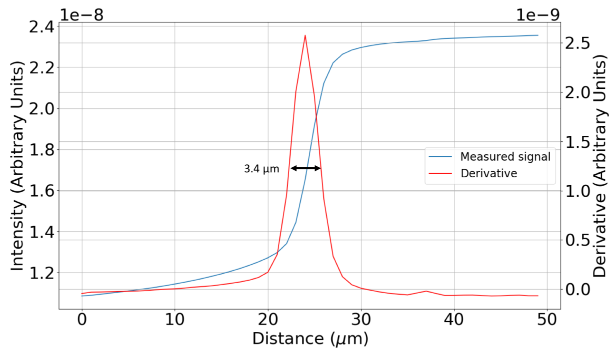

Figure 3: Example of a spatial resolution measurement for the *Al FZP of FUHRIx2 using the sharp edge method for a FZP-blade distance of 253 mm, an energy of 1850 eV.*

.

Resolution measurement of FUHRIx2 FZPs

Figure 4-a shows the results for the Al FZP at a photon energy of 1852 eV. At a FZP-blade distance of 253 mm, a minimum FWHM of (3.4 ±0.3) µm was achieved. In Figure-b the resolution measurement at different energies for the Al FZP are shown for a FZP-blade distance of 253 mm. A ±5 eV variation of the energy induces a spatial resolution variation of a factor x2.

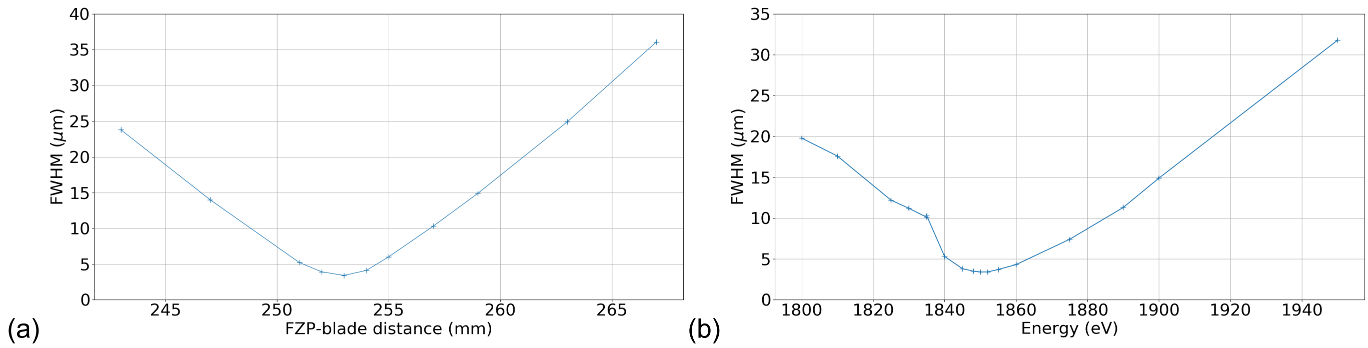

Figure 4: (a) Al FZP resolution as a function of the FZP-blade distance for a photon energy of 1852 eV. (b) Al FZP resolution as a function of the photon energy at best focus for 1852 eV.

As both FZP were placed on the same support the resolution of the Ti FZP was also measured at 253 mm distance from the blade. Resolution of 5 µm was obtained for the Ti FZP and remain stable within at least ±25 eV energy range around the energy of 4700 eV.

2. ML Mirror reflectivity measurements

The components of the multilayer mirrors were deposited by Axo-Dresden[12]. The thickness of each layer can be calculated from the X-ray reflective peaks according the Bragg formula.

The "Al" ML mirror consists of 50 pairs of Pd/B_4C layers (2.6 nm/2.5 nm). The measured and calculated reflectivity curves are compared on Figure 5-a using a Debye Waller roughness of 0.65 nm.

The "Ti" ML mirror is made of 60 stacks of Mo/Si periodical layers. The measured reflectance versus photon energy at 1.975° grazing angle is shown on *Figure 5*-b. The theoretical reflectance (dashed curve) was calculated by the XRV software[16,17], considering a 0.6 nm mean interface substrate layer. From the fitting of the experimental results, we obtain the interface roughness of 0.4 nm.

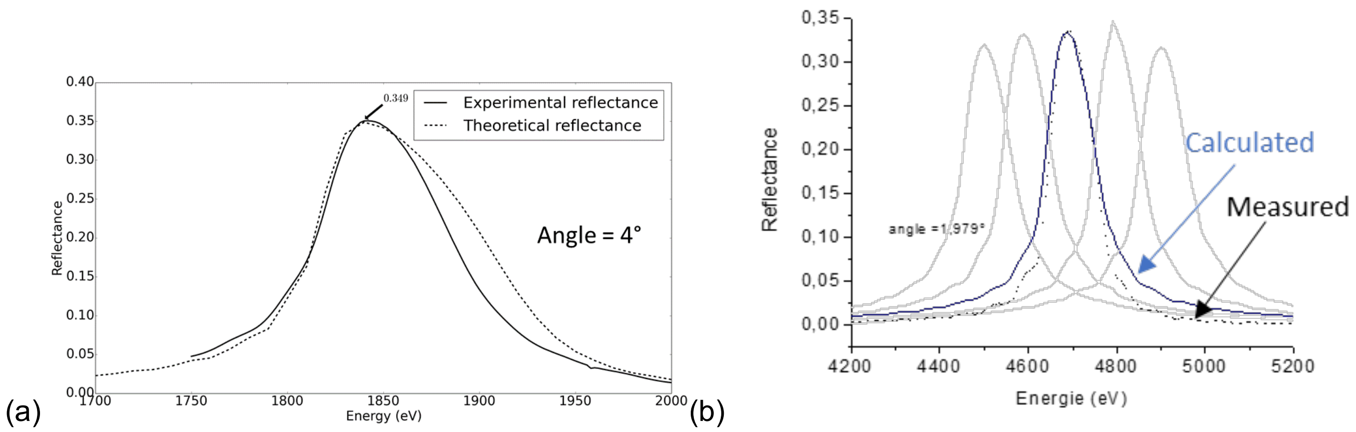

Figure 5: (a) "Al" FZP ML mirror reflectance. (b) "Ti" FZP ML mirror reflectance.

IV. Metrology on a laser facility

The EQUINOX laser facility[13, 14] features a 800 nm-wavelength Ti:sapphire laser producing 0.3 J pulses, focused by an off-axis parabola. The laser pulse duration can be adjusted from 80 fs to 30 ps. As the focal spot diameter is about 50 µm, the irradiance on a flat solid target varies between 10^{14} and 10^{17} W/cm^2, and mostly produces X-rays in the 100 eV – 2 keV range. The laser can operate at 10 Hz for signal accumulation.

The experimental set-up used was the same as that described in ref. [7] and is shown on Figure 6. Our X-ray source is created by irradiating a large Ti or Al foil target with the laser beam. We placed a gold grid (10 µm/40 µm periods) at a distance *d* from the source, the FZP at a distance *p* from the grid and a CCD camera at a distance *q* from the FZP.

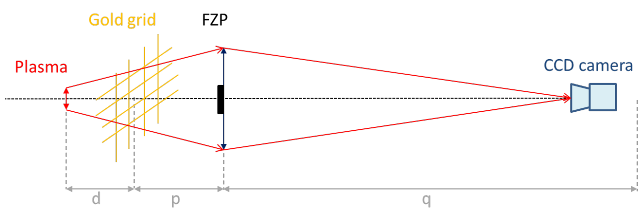

Figure 6: Generic experimental set-up

Using a ML mirror in combination with the FZP selects a specific photon energy band and the corresponding focal distance (Eq. 1). However, in this experiment the geometrical constraints did not allow us to use a ML mirror, this absence caused the whole spectrum to be integrated, thus degrading the resolution significantly. The following resolution measurements must thus be considered as an upper limit. For an optimal result in this situation, the best focusing distance is that of the average energy across the whole spectrum. In the Al case, this average is at 1630 eV, leading to a 222 mm focal distance. For the Ti spectrum, with our experimental conditions, the average is close to the Heα lines (4726.7 eV and 4749.2 eV) thus the focal distance is 250 mm (see *Table 1*).

For each configuration we calculated the p distance with the thin lens formula:

$$\frac{1}{f} = \frac{1}{p} + \frac{1}{q} \quad (2)$$

1. Resolution measurements

Target	*Number of shots*	*Filters*	*d (mm)*	*p (mm)*	*q (mm)*	*q/p*	*q/(d+p)*	*Resolution*	*Contrast*
Al (a)	100	MylarAl (2 µm/0.15 µm) Be (10 µm)	185	243	2782	11.4	6.5	(5.4±1) µm	24%
Ti (b)	100	Ti (8 µm) Be (10 µm)	153.3	274.7	2782	10.1	6.5	(7.5±1) µm	20%

Table 2: Resolution measurements experiment parameters for the Al and Ti configurations.

The signal is collected with a Princeton CCD camera, with a pixel size of 13.5 µm X 13.5 µm by accumulating 100 shots (Figure 7).

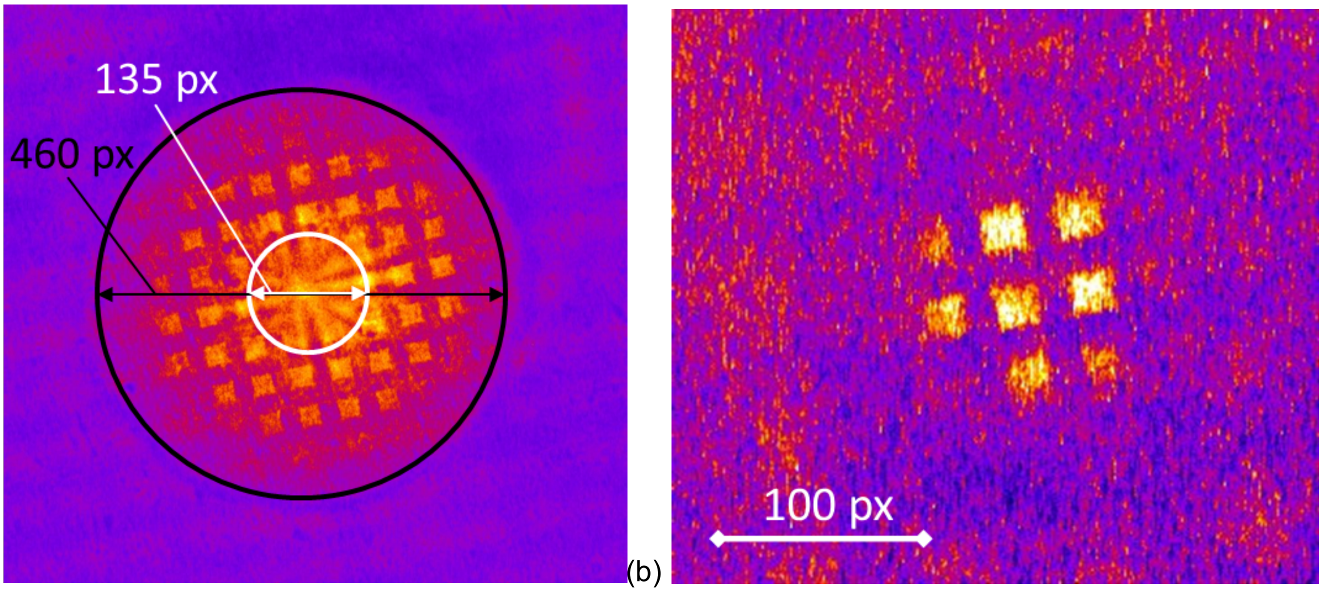

(a) (b)

Figure 7: FUHRIx2 grid radiography image realized at the EQUINOX facility for the (a) Al and (b) Ti given in Table 2.

Note that, for the Al configuration (Figure 7-a), the area inside the white circle is strongly affected by the FZP beam stop. The grid is located relatively far from the plasma to allow a large field of view, but this reduce the photon flux and add diffractions effect on the beam stop, creating the "converging" effect in the white circle of Figure 7-a. The average value of the resolution measured using the sharp edge method is (5.4±1) µm with a mean 24% contrast defined as*: (highest signal - lowest signal)/(highest signal + lowest signal)*. To estimate the effect of an error made on the FZP position, to reproduce this situation we did two resolutions measurement with the grid out of focus (-4 mm and +3 mm). In both case, we measured an average of (7.3±1) µm resolution with a 26% contrast.

For the Ti configuration, the resolution measured here is (7.5±1) µm with a 20% contrast. This suggests that the quality of the Ti FZP is slightly lower than the Al, which confirms the measurement made in Part. III.1. However, the value differences Part III. and Part IV. are likely influenced by the non-monochromaticity of the x-ray source. As in the latter measurement there are no spectral selection, all the energies are being detected on the CCD camera adding more background and blurring to our signal.

V. FUHRIx2 results on a UHI experiment

We implemented FUHRIx2 during a laser-plasma interaction experiment on the LULI2000 facility. When an UHI laser pulse is focused on a thin target (<10 µm), the suprathermal electrons generate a return current which heats a small volume isochorically[15]. One objective of the experiment was to measure the spatial distribution of x-ray emission caused by this hot plasma. These emission lines are temperature dependent, thus providing some insight on the spatial temperature distribution.

The laser delivered pulses from 10 to 15 J in 1.3 ps at a wavelength of 526 nm focused on CH/Ti-Al/CH layered targets (Al and Ti are mixed) with an intensity of 1.6 10^{19} $W.cm^{-2}$. FUHRIx2 was used to investigate the spatial temperature distribution of the aluminum and titanium layer's heated region. The thermal X-ray emission was focused by the FZPs, and the ML mirror, placed in front of the CCD camera, selected the He-like emission from Al and Ti. FUHRIx2 was placed at 22.5° from the target rear normal. The target-FZPs distance was $p = 266.2$ mm and the detector-FZPs distance $q = 4100$ mm corresponding to a magnification around 15.2 and a collection solid angle of 9 10^{-6} sr. The "Al" ML mirror angle was $\theta = 4°$ and the "Ti" ML mirror angle was $\theta = 2°$. Two configurations were used for FUHRIx2. The first was optimized for 2 channels at 1850 eV (Al He_β) and 4700 eV (Ti He_α), while the second was optimized for 2050 eV only (Al H_β). The parameters are summarized in Table 3, and the transmission of FUHRIx2 for two Al configurations are presented on Figure 8 with integrated spectra.

Target	*Filters*	*p* (mm)	*q* (mm)	*q/p*	*Θ*
CH/Ti-Al/CH	PP (10 µm) Be (10 µm)	266.2	4100	15.2	4°(Al) / 2°(Ti) Or 3.65°(Al) / 2°(Ti)

Table 3: Experiment setup parameters.

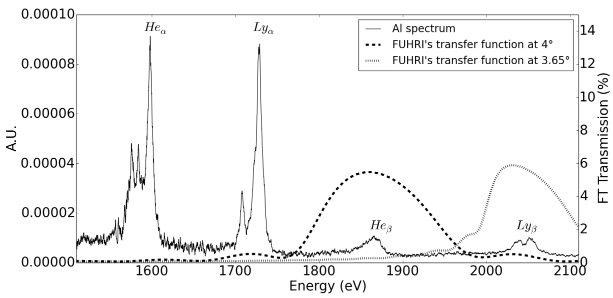

Figure 8: FUHRIx2 Al total transmission for two different mirror angles, superimposed with a typical X-ray spectrum from an UHI experiment.

Unfortunately, we were not able to measure the resolution of each FUHRIx2 channel, we can only give an estimation of the resolution based on our previous paper[7] using FZPs resolution measurement on synchrotron (Part. III) and on a laser facility (Part. IV). Based on the measured resolution of the CCD camera ($\sigma_{CCD} = [2.3 \pm 0.15]$ µm) and the resolution of the FZP ($\sigma_{FPZP-Al} = [1.5 \pm 0.3]\ \mu m$ and $\sigma_{FPZP-Ti} = [5.0 \pm 0.3]\ \mu m$), we obtain a total resolution for each channel of: $\sigma_{Tot-Al} = [2.7 \pm 0.3]\ \mu m$ and $\sigma_{Tot-Ti} = [5.5 \pm 0.3]\ \mu m$.

An example of images obtained with FUHRIx2 is presented on Figure 9-a. We can see the "Ti" image on the left side and the "Al" image on the right side as well as a small part of the direct beam.

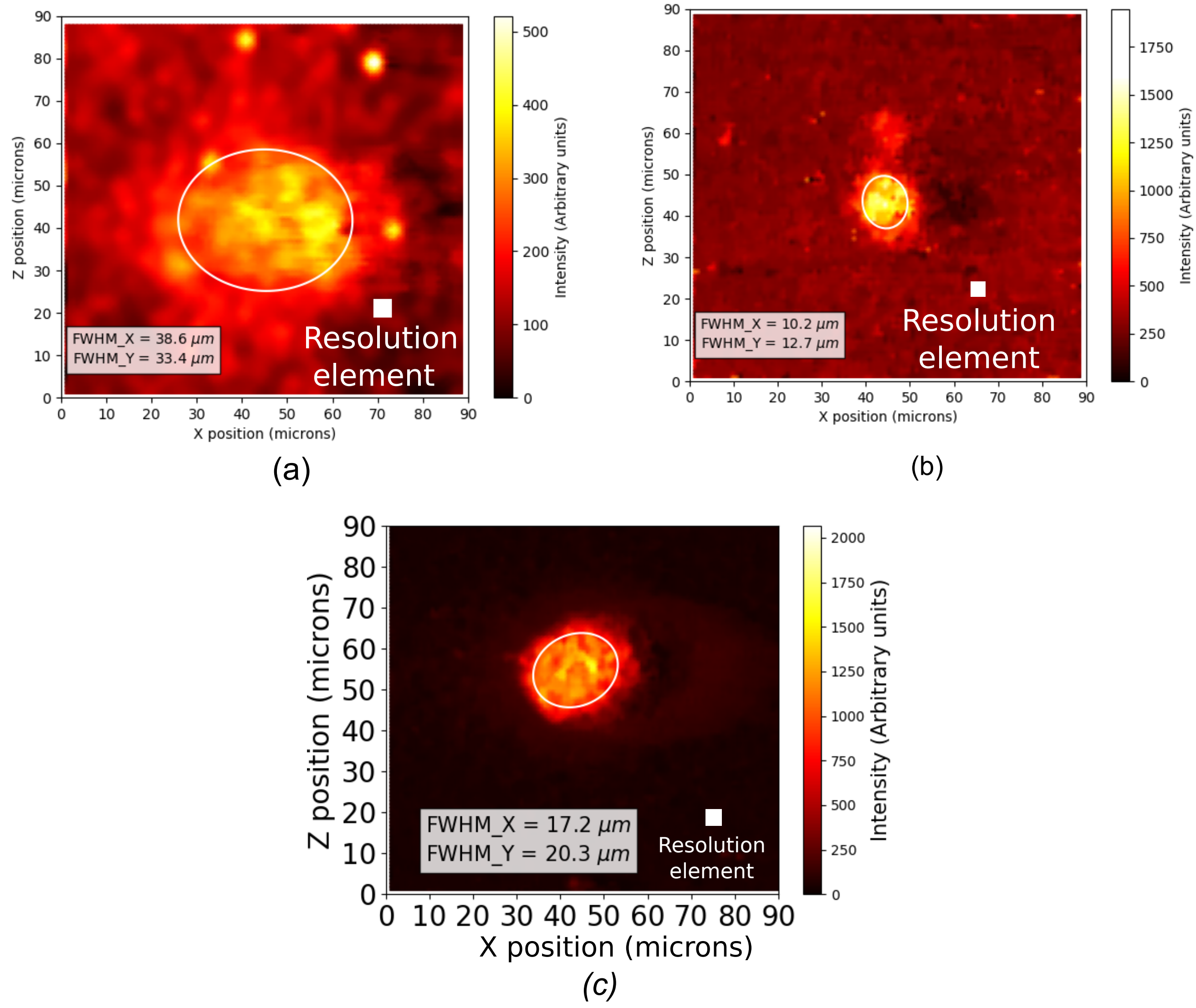

Figure 9: Sample image of FUHRIx2 for a 1.6 10^{19} W.cm^{-2} intensity shot on a mixed target of CH/Al-Ti/CH for (a) the Al FZP at 1850 eV (He_β), (b) the Ti FZP at 4700 eV (He_α), and (c) the Al FZP at 2050 eV (Ly_β).

To compare different lines, we analyzed shots on CH/Al-Ti/CH with the same laser energy (~16 J) and pulse duration. Sample images for each energy are presented on Figure 9-abc. Note that the two images on figure 9bc are from the same shot. The FWHM was estimated using a 2D-Gaussian fit of the images and the results are sown on Table 4. Here we are looking at the same plasma at different energy. For a set of plasma conditions, each emission lines of Al and Ti will have a specific emission zone size and brightness. Thus, we will be able to compare the size and the absolute emission measured with FUHRIx2 with theoretical calculations to verify our emission models. Detailed analysis of all the experimental data will be conducted in another paper. What we can observe here is that the emission area for each X-ray line is smaller for higher X-ray energies. This match corresponds to the heat propagation inside the target: lower temperatures (i.e. lower X-ray energies) are found far from the heat source.

Lines	***Al He_β***	***Al Ly_β***	***Ti He_α***
Resolution (μm)	(2.7 ±0.3)	(2.7 ±0.3)	(5.5±0.3)
E_{FUHRI} ± 50 eV	1850	2050	4700
FWHM (μm)	30-40	16-25	11-15

Table 4: Emission zone size for each energy.

VI. Conclusions

We improved our previous high-resolution X-ray imager by adding an additional measurement channel allowing us to capture simultaneously the size of the emission zone of two different x-ray emission lines with resolutions of (3.4 ±0.3) μm for the Al lines and of (5.5 ±0.3) μm for the Ti line. We proved the versatility of our system by changing the observed energy of one of our channels.

The investigation of chromatism effect on diagnostic performances will be pursued in a future article using x-ray tracing and wave propagation methods.

VII. ACKNOWLEDGMENTS

The authors acknowledge the LULI2000 team, the LULI target lab, as well as Levent Cibik and Swenja Schreiber (both PTB) for their help during the experiments as well as Laboratoire de Photonique et de Nanostructures (LPN-CNRS, Marcoussis, France) lab team for their help in imaging FZP with a scanning electron microscope.

VIII. References

[1]M. Krumrey and G. Ulm,Nucl. Instr. and Meth. A 467-468, 1175 - 1178 (2001)

[2]D. Fuchs, M. Krumrey, P. Müller, F. Scholze and G. Ulm, Rev. Sci. Instrum. 66, 2248 - 2250 (1995)

[3]C. Blancard, Ph. Cossé, G. Faussurier, The Astrophysical Journal, Volume 745, Issue 1, article id. 10, 7 pp. (2012).

[4]M. Tabak, J. Hammer, M. E. Glinsky, et al., 1994. Physics of Plasmas, vol. 1 p. 1626–1634.

[5]LULI2000. *LULI.* www.luli.polytechnique.fr/accueil/les-installations/luli2000.

[6]J. Kirz, J. Opt. Soc. Am. 64, 301-309 (1974).

[7]A. Do, Ph. Troussel et Al., Rev Sci Instrum. 2017 Jan.88(1): 013701.

[8]F A. Jenkins, H.E. White. *Fundamentals of Optics. Chap. 18, Frensel Diffraction.* s.l. : McGraw-Hill Book Compagny (1957).

[9]K. Kamiya, Science of light, pp. Vol. 12, No. 2, p. 35-49 (1963).

[10]*G.* Cauchon, M. Pichet-Thomasset, R. Sauneuf, P. Dhez, M. Idir, M. Ollivier, Ph. Troussel, J.-Y. Boutin and J.-P. Le Breton, Rev. Sci. Instrum., Vol. 69, 3186 (1998).

[11]www.appliednt.com

[12]http://www.axo-dresden.de/

[13]J. P. LeBreton, E. Alozy, J. Y. Boutin, A. Duval, S. Gary, D. Gontier, S. Jasmin, M. Naudy, C. Reverdin, R. Rosch et al., Rev. Sci. Instrum. 77, 10F530 (2006).

[14]Ch. Reverdin, M. Paurisse, T. Caillaud, P. Combis, A. Duval, D. Gontier, D. Husson, Ch. Rubbelynck, and C. Zuber, Rev. Sci. Instrum. 79, 10E932 (2008).

[15] V. Dervieux, B. Loupias, S. Baton, *et al.* 12-17, 2015, HEDP, Vol. 16.

[16]T. Moreno, Software X-ray Vision applied by Caminotec, Paris, France

[17]L. G. Parratt, Phys. Rev. 95, 2 (1954).